IEICE Communications Express, Vol.12, No.10, 568–571

ComEX

LETTER

A placement method of ground stations for optical satellite communications considering cloud attenuation

Thanh V. Pham [1, a)], **Hiroya Yamano** [2], **and Ishihara Susumu** [1]

Abstract This letter studies a placement method of optical ground stations (OGSs) to realize site diversity in optical satellite-to-ground communications under cloud attenuation. Using a meteorological ERA-Interim database, the monthly average cloud attenuation over Japan during 2018–2022 is calculated. Based on the obtained results, a set of candidates for the OGS is proposed, including places with the lowest attenuation, major cities, and a JAXA observatory station. Then, a greedy heuristic method is presented to determine a sub-optimal set of OGSs. Simulation results reveal that sufficiently high system availabilities are achieved when site diversity is performed from the proposed set of candidates.

Keywords: optical satellite communications, cloud attenuation, site diversity

Classification: Satellite communications

1. Introduction

The current satellite-to-ground communications extensively use radio frequency (RF) bands, typically between the L-band (1–2 GHz) and the Ka-band (26–40 GHz). However, the ever-increasing demand for high data rates and traffic volume has spurred the necessity of moving to optical frequencies [1]. In addition to offering much larger bandwidth compared to their RF counterparts, optical satellites also enable lightweight transceivers and higher security due to the high directionality of optical beams [2].

It is well-known that the optical signal propagating through the atmosphere is distorted by various phenomena, among which clouds are the main source of attenuation. As a matter of fact, attenuation due to clouds can be as high as 600 dB/km [3], rendering the communication link outage. In this regard, site diversity is considered the most promising solution to tackle cloud attenuation and improve the system's availability.

The idea of site diversity is to deploy multiple optical ground stations (OGSs) with small cloud cover correlation so that high availability of a communication link can be guaranteed. Hence, the location and selection of OGSs are crucial for achieving this purpose. Given the locations of existing OGSs (or a set of GS candidates), several studies investigated different optimization methods to find the optimal OGS network [3, 4, 5]. These works considered that a link blockage event occurs as long as clouds are present. This assumption, however, is rather too conservative as the transmission is still possible under low cloud-induced attenuation. In fact, the study in [6] evaluated the link availability considering the combined impact of atmospheric turbulence and cloud attenuation.

In this letter, we first analyze the average monthly cloud attenuation over Japan's main islands during a 5-year period (2018–2022) using the ERA5 database [7]. Each month, the location with the lowest average attenuation is then selected as a candidate for OGS. In addition to these locations, urban areas and existing space facilities are also preferable in practice due to the ease of accessibility and maintenance. Hence, a list of major cities and an existing JAXA optical observatory station are considered possible candidates as well. From the set of chosen candidates, the optimal OGS network can be found via an exhaustive search, which, however, is computationally expensive. We, therefore, present a greedy heuristic method to determine a sub-optimal set of OGSs. Simulation results show significant reductions in cloud attenuation when OGSs are selected from the proposed set of possible candidates.

2. Cloud attenuation model

In this section, we describe the cloud attenuation model proposed in [8], which is then used to analyze the ERA5 data. The attenuation induced by the water particles in the clouds is a function of the optical wavelength λ (μm) and is given by

$$A(\lambda) = \int_{l_0}^{l_{\max}} \beta_{\text{ext}}(\lambda) \mathrm{d}l, \quad \text{(dB)} \tag{1}$$

where $\beta_{\text{ext}}(\lambda)$ is the volume extinction coefficient while l_0 (km) and $l_{\max}$ (km) are the lower and upper limits of the slant path through the cloud formation. The volume extinction coefficient is calculated by

$$\beta_{\text{ext}}(\lambda) = 4.343 \times 10^3 \int_0^{\infty} \sigma_{\text{ext}}(r, \lambda) n(r) \mathrm{d}r, \quad \text{(dB/km)} \tag{2}$$

where $\sigma_{\text{ext}}(r, \lambda)$ (μm^2) is the extinction cross coefficient, $n(r)$ (μm^{-1}/cm^3) is the particle size distribution of cloud droplets, and r (μm) the radius of the cloud droplet. The extinction cross coefficient can be estimated using

$$\sigma_{\text{ext}}(r, \lambda) = \frac{36\pi\nu\kappa}{Z} \frac{V}{\lambda}, \quad (\mu\text{m}^2) \tag{3}$$

[1] Dept. of Mathematical and Systems Engineering, Shizuoka University, 3–5–1 Johoku, Naka-ku, Hamamatsu, Shizuoka 432–8011, Japan

[2] Kioxia Holdings Corporation, Japan

[a)] pham.van.thanh@shizuoka.ac.jp

DOI: 10.23919/comex.2023XBL0092
Received June 15, 2023
Accepted July 21, 2023
Publicized September 22, 2023
Copyedited October 1, 2023

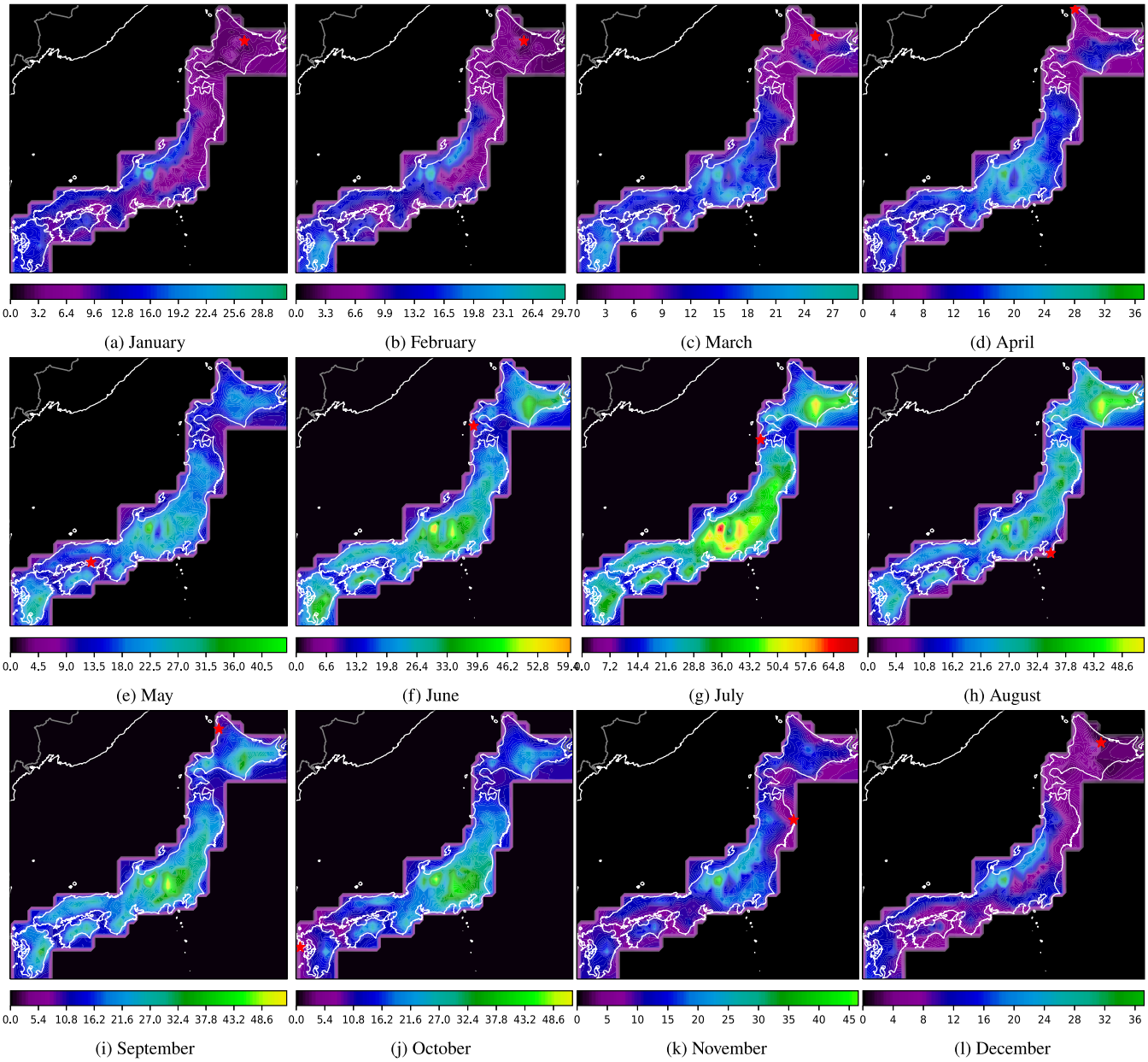

Fig. 1 Average monthly cloud attenuation over Japan's main islands.

with $Z = (\nu^2 + \kappa^2)^2 + 4(\nu^2 - \kappa^2 + 1)$ and $V = \frac{4}{3}\pi r^3$ is the volume of the cloud droplet. Here, κ and ν are wavelength-dependent parameters, which are 8.55×10^{-5} and 1.317, respectively, at wavelength $\lambda = 1.6\,\mu$m [9]. The particle size distribution of cloud droplets can be modelled by the four-parameter modified gamma function as

$$n(r) = g \times r^a \times \exp(-b \times r^\gamma), \tag{4}$$

where a, b, and γ vary with cloud types, which in turn can be categorized based on the average vertical extent. Typical values of a, b, and γ are associated with different cloud types, for example, $(a, b, \gamma) = (3, 0.5, 1)$ for cumulonimbus and cumulus, (2, 0.425, 1) for nimbostratus, and (2, 0.6, 1) for stratus [8]. Also, g is given by

$$g = \frac{3 \times \gamma \times b^{a+4/\gamma} \times w}{4 \times \pi \times \rho_w \times \Gamma((a+4)/\gamma)}, \tag{5}$$

where w (g/m^3) is the the cloud liquid water content, p_w (g/cm^3) is the water density, and $\Gamma(\cdot)$ is the gamma function.

3. Analysis of cloud attenuation over Japan

Firstly, we extract the cloud liquid water content data from the ERA5 database over the geographical area from 31°N to 45°45′N and from 129°30′E to 145°30′E. These latitudes and longitudes correspond to the southernmost, northernmost, westernmost, and easternmost of Japan's four main islands. The data is collected with a temporal resolution of 1 hour and spatial resolution of 0.255° × 0.255°. Using (1)–(5), the average monthly cloud attenuation is calculated and shown in Fig. 1, where places with the lowest average attenuation are marked by a red star. More specifically, the locations of these places are Engaru (January and February, Hokkaido, 43°45′N 143°15′E), Engaru (March and December, Hokkaido, 44°N 143°15′E), Wakkanai (April, Hokkaido, 45°30′N 141°45′E), Shodoshima (May,

Kagawa, 34°30′N 134°15′E), Yakumo (June, Hokkaido, 42°N 140°E), Matsumae (July, Hokkaido, 41°15′N 140°E), Kamogawa (August, Chiba, 35°N 140°15′E), Embetsu (September, Hokkaido, 44°45′N 141°45′E), Nagasaki (October, Nagasaki, 32°45′N 129°45′E), and Miyako (November, Iwate, 39°45′N 142°E).

While there are such OGSs in Japan, due to better-seeing conditions (i.e., to minimize the effect of atmospheric turbulence, which is the second significant attenuation factor after clouds), possible site candidates should also be close to astronomical observatories on a mountaintop, for example, the JAXA optical observatory station in Ina (Nagano, 36°N 138°15′E). Furthermore, for convenient accessibility and maintenance, major cities are possible locations for the OGSs as well. Therefore, ten major cities, including Sapporo (Hokkaido, 43°15′N 141°30′E), Sendai (Miyagi, 38°15′N 141°E), Tokyo (35°45′N 139°45′E), Niigata (Niigata, 37°45′N 139°E), Hamamatsu (Shizuoka, 34°45′N 137°45′E), Nagoya (Aichi, 35°15′N 137°E), Hiroshima (Hiroshima, 34°30′N 132°30′E), Fukuoka (Fukuoka, 33°39′N 130°30′E), Kagoshima (Kagoshima, 31°30′N 130°30′E) are also chosen to form a set of 21 possible candidates for the OGSs.

4. Optical ground station selection method

From the set of the above-mentioned 21 location candidates, one can exhaustively try all possible subsets and calculate the resulting attenuation reduction. If the number of candidates is large, the exhaustive search may not be practical due to its high computational complexity (i.e., the number of non-empty combinations is $2^N - 1$ with N being the number of candidates). Hence, we are interested in a greedy heuristic algorithm that strives for a tradeoff between performance and computational time. To this end, let $\mathcal{S} = \{G_1, G_2, \ldots, G_{21}\}$ and $\mathcal{G}$ be the set of all possible candidates described in the previous section and the set of selected OGSs, respectively. At the beginning of the algorithm, $\mathcal{G} = \emptyset$ is set. Then, at each time instant t, the OGS with the lowest cloud attenuation (denoted as $G_{\min,t}$) is added to $\mathcal{G}$, i.e., $\mathcal{G} \leftarrow \mathcal{G} \cup G_{\min,t}$, until a convergence condition is met. Here,

$$G_{\min,t} = \arg \min_{G_i \in \mathcal{S} \setminus \mathcal{G}} A_{i,t}(\lambda), \tag{6}$$

where $A_{i,t}(\lambda)$ is the cloud attenuation at the OGS G_i at time instant t.

5. Simulation results and discussion

As the JAXA optical observatory station is already in operation, it is reasonable to select it as the starting point of the greedy heuristic algorithm. The algorithm terminates when adding more OGSs does not further reduce the average cloud attenuation. The resulting selection of OGSs from the greedy heuristic algorithm for each year are tabulated in Table I, which is on top of the following page.

It is seen that, except in 2018, the attenuation converges when the number of OGSs reaches about 11 to 13. This might be because, from the calculation of the average monthly cloud attenuation, there are several

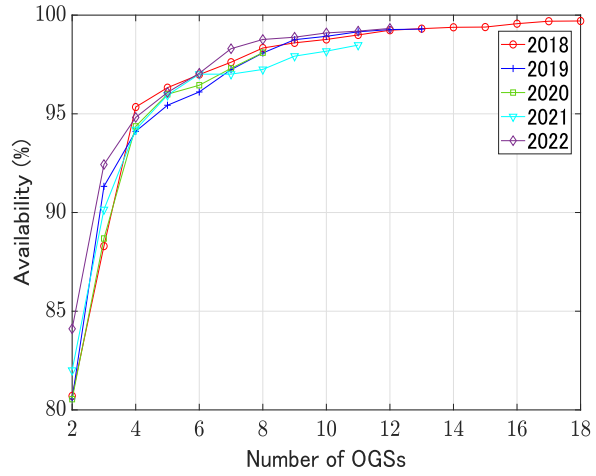

(a) 5 dB link budget margin.

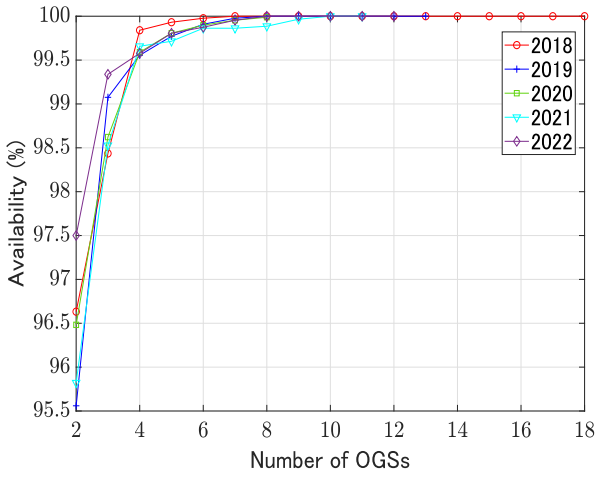

(b) 20 dB link budget margin.

Fig. 2 System availability using site diversity.

candidates whose corresponding cloud attenuations are not much different (e.g., Shodoshima (7.987 dB)-Yakumo (7.971 dB)-Embetsu (7.767 dB) and Wakkanai (5.098 dB)-Miyako (5.506 dB)). Therefore, adding one or more OGSs, which have almost the same attenuation as the one that has been selected, does not significantly decrease the attenuation further.

From the selected OGSs in Table I, the system availabilities respective to the number of OGSs are illustrated in Figs. 2(a) and 2(b) assuming 5 dB and 20 dB link budget margin, respectively. In the case of 5 dB, it can be achieved by increasing the transmit power or employing a larger telescope at the OGS, while it may only possible to obtain the 20 dB margin by reducing the data rate. In both settings, as the number of OGSs increases, significant improvements in system availability are observed. At the target of 99% availability, it is seen that at least 12 OGSs are required in the case of the 5 dB link budget margin while only 4 OGSs are needed when the 20 dB link budget margin is available. This demonstrates that, in the deployment of practical systems, care should be specifically given to the available link budget margin as it considerably affects the required number of OGSs so that a desirable system availability can be attained.

Table I Selection of OGSs.

Step	2022	2021	2020	2019	2018
1	Ina	Ina	Ina	Ina	Ina
2	Embetsu	Yakumo	Embetsu	Nagasaki	Embetsu
3	Shodoshima	Embetsu	Kamogawa	Sapporo	Matsumae
4	Niigata	Kagoshima	Nagasaki	Engaru (January)	Nagasaki
5	Wakkanai	Engaru (March)	Sendai	Tokyo	Engaru (January)
6	Tokyo	Wakkanai	Tokyo	Niigata	Hamamatsu
7	Yakumo	Engaru (December)	Sapporo	Wakkanai	Niigata
8	Miyako	Engaru (January)	Yakumo	Kamogawa	Tokyo
9	Sapporo	Sendai		Yakumo	Kagoshima
10	Kagoshima	Osaka		Hiroshima	Yakumo
11	Matsumae	Tokyo		Shodoshima	Sendai
12	Hiroshima			Engaru (March)	Shodoshima
13				Embetsu	Miyako
14					Engaru (March)
15					Fukuoka
16					Wakkanai
17					Kamogawa
18					Hiroshima

6. Conclusion

In this letter, we studied a placement method of OGSs for the implementation of site diversity in optical satellite-to-ground communications. A 5-year cloud data was analyzed to form a set of possible candidates from which a sub-optimal set of OGSs was selected using a greedy heuristic method. Under the setting of 5 dB and 20 dB link budget margin, simulation results revealed that sufficiently high system availabilities are achievable with site diversity using OGSs selected from the proposed method.

References

[1] M. Toyoshima, "Recent trends in space laser communications for small satellites and constellations," *J. Lightw. Technol.*, vol. 39, no. 3, pp. 693–699, 2021. DOI: 10.1109/jlt.2020.3009505

[2] H. Kaushal and G. Kaddoum, "Optical communication in space: Challenges and mitigation techniques," *IEEE Commun. Surveys Tuts.*, vol. 19, no. 1, pp. 57–96, 2017. DOI: 10.1109/comst.2016.2603518

[3] C. Fuchs and F. Moll, "Ground station network optimization for space-to-ground optical communication links," *J. Opt. Commun. Netw.*, vol. 7, no. 12, pp. 1148–1159, 2015. DOI: 10.1364/jocn.7.001148

[4] N.K. Lyras, C.N. Efrem, C.I. Kourogiorgas, and A.D. Panagopoulos, "Optimum monthly based selection of ground stations for optical satellite networks," *IEEE Commun. Lett.*, vol. 22, no. 6, pp. 1192–1195, 2018. DOI: 10.1109/lcomm.2018.2819174

[5] S. Gong, H. Shen, K. Zhao, R. Wang, X. Zhang, T. De Cola, and J.A. Fraier, "Network availability maximization for free-space optical satellite communications," *IEEE Wireless Commun. Lett.*, vol. 9, no. 3, pp. 411–415, 2020. DOI: 10.1109/lwc.2019.2958804

[6] T.V. Nguyen, H.D. Le, T.V. Pham, and A.T. Pham, "Link availability of satellite-based FSO communications in the presence of clouds and turbulence," *IEICE Commun. Express*, vol. 10, no. 5, pp. 206–211, 2021. DOI: 10.1587/comex.2021xbl0009

[7] H. Hersbach *et al.*, "ERA5 hourly data on single levels from 1940 to present," Copernicus Climate Change Service (C3S) Climate Data Store (CDS).

[8] N.K. Lyras, C.I. Kourogiorgas, and A.D. Panagopoulos, "Cloud attenuation statistics prediction from Ka-band to optical frequencies: Integrated liquid water content field synthesizer," *IEEE Trans. Antennas Propag.*, vol. 65, no. 1, pp. 319–328, 2017. DOI: 10.1109/tap.2016.2630602

[9] G.M. Hale and M.R. Querry, "Optical constants of water in the 200-nm to 200-μm wavelength region," *Appl. Opt.*, vol. 12, no. 3, pp. 555–563, 1973. DOI: 10.1364/ao.12.000555